Research Square

Preprints are preliminary reports that have not undergone peer review.
They should not be considered conclusive, used to inform clinical practice,
or referenced by the media as validated information.

Brain MRI of Dystroglycanopathy Patients in a Chinese Pediatric Cohort: Genotype-Specific Neuroimaging Signatures and Neurodevelopmental Correlates

Danyu Song
Peking University First Hospital
Yidan Liu
Beijing Children's Hospital
Shunfeng Lin
Renmin University of China
Jihang Luo
Beijing Children's Hospital
Xiaona Fu
Beijing Children's Hospital
Haipo Yang
Peking University First Hospital
Ying Zhu
Peking University First Hospital
Hui Xiong
xionghui@bch.com.cn

Beijing Children's Hospital

Research Article

Keywords: Dystroglycanopathy, Neuroimaging, Genotype-phenotype correlation, Cerebellar dysplasia

Posted Date: October 29th, 2026

DOI: https://doi.org/10.21203/rs.3.rs-11320201/v1

License: This work is licensed under a Creative Commons Attribution 4.0 International License.
Read Full License

Additional Declarations:

No competing interests reported.

Tables are available in the Supplementary Files section.

Brain MRI of Dystroglycanopathy Patients in a Chinese Pediatric Cohort: Genotype-Specific Neuroimaging Signatures and Neurodevelopmental Correlates

Danyu Song[1], Yidan Liu[2], Shunfeng Lin[3], Jihang Luo[1], Xiaona Fu[2], Haipo Yang[1], Ying Zhu[4,*], Hui Xiong[2,*]

[1]Department of Pediatrics, Peking University First Hospital, Beijing, China

[2]Department of Neurology, Beijing Children's Hospital, Capital Medical University, National Center for Children's Health, Beijing, China

[3]Statistical Consulting Center, Renmin University of China

[4]Department of Radiology, Peking University First Hospital, Beijing, China

*Corresponding author:

Hui Xiong, Department of Neurology, Beijing Children's Hospital, Capital Medical University, National Center for Children's Health, Beijing, China. Email: xh_bjbj@163.com; xionghui@bch.com.cn

Ying Zhu, Department of Radiology, Peking University First Hospital, Beijing, China. Email: imazhu@bjmu.edu.cn

Funding

This work was supported by Beijing Natural Science Foundation (7254435), National Natural Science Foundation of China (No. 82471430) and Open Research Fund Program of MOE Key Laboratory of Major Diseases in Children (Capital Medical University), Ministry of Education (No. BCH-MOE-2025-9).

Conflict of interest

No financial or non-financial benefits have been received or will be received from any party related directly or indirectly to the subject of this article.

Data Available Statement

Anonymized data from participants will be available on request.

Ethics Approval

The research protocol was approved by the Ethics Committee of Peking University First Hospital.

Contributors' statement:

Danyu Song and Hui Xiong conceptualized and designed the study. Danyu Song, Yidan Liu, Shunfeng Lin, Jihang Luo, Xiaona Fu, Haipo Yang, and Ying Zhu contributed to data acquisition, analysis, and interpretation. Shunfeng Lin performed the statistical analysis and contributed to data analysis and interpretation. Danyu Song and Yidan Liu drafted the manuscript. Hui Xiong, Ying Zhu, Shunfeng Lin, Jihang Luo, Xiaona Fu, and Haipo Yang critically revised the manuscript for important intellectual content. All authors approved the final version to be published and agree to be accountable for all aspects of the work. Hui Xiong and Ying Zhu are the guarantors of this paper and take responsibility for the integrity of the work as a whole, from inception to published article.

Declaration of generative AI and AI-assisted technologies in the writing process:

The authors declare that no generative AI or AI-assisted technologies were used in the writing process of this manuscript.

Abstract

Objective: To delineate clinical-genetic-neuroimaging correlations in a Chinese cohort of patients with dystroglycanopathy (DGP).

Methods: This observational cohort study enrolled 90 genetically confirmed DGP patients. Brain MRI was available for 63 patients; 38 high-quality scans underwent blinded phenotyping. Patients were classified into Group 1 (combined supratentorial and infratentorial malformations), Group 2 (isolated infratentorial malformations), and Group 3 (normal/non-specific findings). Clinical assessments included motor milestones, intellectual disability, expressive language, receptive language, and epilepsy. Spearman's correlation and network analyses were performed.

Results: The genetic spectrum included *POMGNT1* (12), *CRPPA* (7), *POMT1* (6), *FKRP* (5), *FKTN* (4), *POMT2* (2), and *B3GALNT2* (2). Commonest MRI abnormalities were cerebellar dysplasia (71%), brainstem hypoplasia (63%), and cerebellar microcysts (58%). Group 1 n=19 had severe intellectual disability (100%) and global motor delay; 63% were preverbal/early verbal, 32% had limited phrases, and only 5% achieved basic conversation; epilepsy occurred in 53% and mortality in 16%. Group 2 n=9 had milder intellectual (56%) and language impairment (44%); 67% achieved basic conversation, 89% comprehended simple commands, and epilepsy occurred in 33%. Group 3 n=10 had the mildest phenotype; no epilepsy or mortality occurred, 80% achieved basic conversation, and 100% comprehended simple commands. Imaging severity correlated strongly with clinical phenotype $\rho=0.756$,$P<0.001$. Expressive language was the most connected clinical hub, but partial correlations adjusting for supratentorial lesions rendered infratentorial associations non-significant (all $P>0.05$). Receptive language deficits correlated specifically with lissencephaly $\rho=0.62$,$P<0.001$; cerebellar dysplasia independently correlated with epilepsy (partial $r=0.351$, $P=0.033$). Genotype dictated distinct correlation spectra: *POMGNT1* almost exclusively drove Group 1 (83%); *CRPPA* uniformly showed cerebellar dysplasia; *POMT1/POMT2* exhibited "functional-structural dissociation"; *FKRP* showed the broadest heterogeneity and weakest imaging-clinical alignment.

Conclusions: Receptive language deficit is highly specific and strongly associated only with lissencephaly, whereas expressive language is the most widespread and sensitive clinical indicator. Genotype-guided neuroimaging assessment is essential for precise prognostication.

Keywords: Dystroglycanopathy; Neuroimaging; Genotype-phenotype correlation; Cerebellar dysplasia

Introduction

Dystroglycanopathy (DGP) represents a clinically heterogeneous group of muscular dystrophies caused by aberrant glycosylation of α-dystroglycan.(1) Based on clinical severity, the disorder is classified into three main subtypes: Type A (severe form) manifests as congenital muscular dystrophy with significant brain and ocular abnormalities, including Walker-Warburg syndrome (WWS), muscle-eye-brain disease (MEB), and Fukuyama congenital muscular dystrophy (FCMD); Type B (intermediate form) presents as congenital muscular dystrophy with or without intellectual disability; and Type C (mild form) is characterized by limb-girdle muscular dystrophy without brain or ocular involvement.(2, 3)

Characteristic neuroimaging findings of DGP include cobblestone lissencephaly, cerebellar dysplasia, brainstem hypoplasia, and cerebellar cysts.(4, 5) However, the precise relationships between specific imaging patterns, clinical outcomes, and underlying genotypes remain incompletely understood, particularly in Asian populations.This study retrospectively analyzed brain MRI records from a Chinese cohort comprising 63 genetically confirmed DGP cases, including 38 available scans. The research aims to systematically delineate clinical-genetic-neuroimaging correlations, with the objectives of refining diagnostic accuracy and improving prognostic stratification.

Patients and Methods

Patients and clinical assessments

This cohort study enrolled 90 genetically confirmed dystroglycanopathy (DGP) patients who were followed up at the Pediatric Department of Peking University First Hospital or Beijing Children's Hospital. Brain magnetic resonance imaging (MRI) records or reports were available for 63 of these patients. Among them, raw MRI scans were retrievable for 38 patients, which constituted the core imaging cohort for blinded, detailed phenotyping and served as the primary group for in-depth clinico-radiological and genotype-imaging correlation analyses. For the remaining 25 patients, only descriptive MRI reports from medical records were accessible; these cases were included solely for supplementary analysis of the distribution between clinical subtypes and imaging patterns (see Section 3.3). All participants underwent comprehensive clinical assessments, including evaluation of motor function, intellectual development, communication, comprehension, history of seizures, treatment and brain MRI. Follow-up time was calculated from the date of the patient's clinic visit to the date of loss to follow-up or the last follow-up. The last follow-up date was March 2026.

Ethics approval and consent to participate:

The research protocol was approved by the Ethics Committee of Peking University First Hospital. Written informed consent to participate was obtained from all participants or, for children under 16 years of age, from their parents or legal guardians.

Communication Assessment and Classification: Due to significant language delays in our cohort with intellectual disabilities, we assessed foundational communication and social responsiveness using the "Communication" subscale of the Social Life Abilities Scale (S-M). The evaluation included three domains: (1) Social Responsiveness: responding to one's own name [Q1]; reacting to unfamiliar persons [Q2]; (2)Expressive Language Development: use of single words [Q3, e.g., "mama", "bye-bye".]; production of two-word phrases [Q4, e.g., "go outside"]; use of social phrases [Q5, e.g., "thank you"]; spontaneous description of events [Q6]); and Receptive Language (comprehension of simple commands [Q7, e.g., "bring the object"]). Based on this profile, expressive language was classified hierarchically: A) Preverbal/Early Verbal (failed single-word use, Q3), B) Limited Phrasal Language (passed Q3-Q5 but failed spontaneous description, Q6), and C) Basic Conversational Ability (passed Q6). Comprehension (Q7) and social responsiveness (Q1, Q2) were analyzed separately.

Brain Magnetic Resonance Imaging

Brain MRI scans were independently reviewed by two investigators blinded to clinical and genetic data. To reduce potential bias in retrospective data collection and imaging assessment, imaging reviewers were blinded to clinical and genetic data, and clinical data were extracted by trained researchers using a standardised form. The imaging features assessed included cortical malformations (cortical thickening, polymicrogyria-like, or lissencephaly), cerebellar abnormalities (cysts, vermian or hemispheric hypoplasia/dysplasia), brainstem hypoplasia, white matter changes, ventriculomegaly, and other structural anomalies. Based on the presence of supratentorial and/or infratentorial involvement, patients were categorized into three groups: Group 1-severe malformations with both cortical and infratentorial involvement (cerebellum and/or brainstem); Group 2-malformations confined to the infratentorial region; Group 3-normal MRI or nonspecific findings (isolated white matter changes or ventriculomegaly). A comparison between our imaging-based classification and current clinical-imaging or imaging-based classifications is presented in Table S1. To quantify brain involvement, composite scores (0-3) were generated for supratentorial (cortical thickening, polymicrogyria, lissencephaly) and infratentorial

(cerebellar dysplasia, cysts, brainstem hypoplasia) regions by summing the presence (1 point each) of these features.

Statistical Analysis

Statistical analyses were performed using R software. Continuous variables, which were confirmed to be non-normally distributed by the Shapiro-Wilk test, were expressed as median (minimum-maximum). The Kruskal-Wallis test was used to compare differences in motor milestones (age at head control, sitting, and walking) among the three imaging groups. The chi-squared test or Fisher's exact test was employed to compare differences in the frequencies of intellectual disability, language function grades, epilepsy, and mortality among the three groups. Spearman's rank correlation analysis was used to assess the correlation between clinical severity types (A/B/C) and imaging groups (1/2/3), as well as the correlation between clinical severity scores and imaging grades within each genotype. Weighted Kappa analysis was performed to quantify the agreement between clinical classification and imaging classification. In genotype-phenotype analysis, the chi-squared test was used to compare the composition ratios of different genotypes across imaging groups. Spearman correlation and partial correlation (controlling for supratentorial score) were performed. A P-value < 0.05 was considered statistically significant. Missing data were not imputed or statistically calculated; analyses were based on available observed data.

Results

Among the 90 genetically diagnosed DGP patients, 63 had available MRI reports/records. Of these, the original MRI scans were retrievable and subjected to detailed, blinded review for 38 patients, who constituted the core cohort for subsequent in-depth phenotyping and statistical analysis.

3.1 Clinical Characteristics by Neuroimaging Group

The clinical and brain images characteristics of the 38 patients, stratified by the three-tier imaging severity classification, are summarized in Table 1 and Table 2.

Group 1 (Severe Cortical-Infratentorial Malformations, n=19) presented with universal severe intellectual disability (100%, 19/19) and global motor delay. All achieved head control by a median age of 0.65 years (0.3-5), 84% (16/19) sat independently by 1.3 years (0.5-5), and 47% (9/19) walked independently by a median of 3 years (1.7-9), which was significantly later than other groups (Figure 2a and 2b). Language assessment revealed severe impairment: 63% (12/19) were preverbal/early verbal (Grade A; one unresponsive to name), 32% (6/19) had

limited phrases (Grade B), and only 5% (1/19) achieved basic conversation (Grade C). Overall, 95% (18/19) had significant language impairment, while 79% (15/19) comprehended simple commands (Q7). Epilepsy prevalence was 53% (10/19) and mortality 16% (3/19). Genotypically, *POMGNT1* mutations predominated (53%, 10/19).

Group 2 (Isolated Infratentorial Malformations, n=9) showed milder intellectual and language dysfunction than Group 1. Intellectual disability occurred in 56% (5/9). Motor milestones were achieved earlier: 78% (7/9) attained head control by 0.5 years (0.3-3.5), 89% (8/9) sat by 1 year (0.5-4.5), and 44% (4/9) walked by 1.8 years (1.3-6.5). Language function was better preserved: 11% (1/9, WWS) were Grade A (no name response), 22% (2/9) Grade B, and 67% (6/9) Grade C. Language impairment prevalence was 44% (4/9), and 89% (8/9) comprehended simple commands. Epilepsy occurred in 33% (3/9) and mortality in 22% (2/9). Genetically, *CRPPA* (56%, 5/9) and *POMT1* (33%, 3/9) mutations were most common.

Group 3 (Normal/Non-Specific MRI, n=10) had the mildest phenotype. All achieved head control by 0.3 years (0.3-1.3) and sitting by 0.65 years (0.5-1.5); 70% (7/10) walked independently by 1.5 years (1.2-2.5). No epilepsy or mortality occurred. Intellectual disability was present in 70% (7/10) but was mild. All used simple words: 20% (2/10) were Grade B and 80% (8/10) Grade C; 100% (10/10) comprehended simple commands. Notably, those with intellectual disability exhibited marked deficits in higher cognitive functions (e.g., calculation). Genetically, *FKRP* and *POMT1/POMT2* mutations were equally represented (each 30%, 3/10).

3.2 Spectrum of Brain MRI Abnormalities and Imaging-Based Classification

The detailed review of the 38 MRI scans revealed a distinct spectrum of structural anomalies . Cerebellar dysplasia (71.1%, 27/38), brainstem hypoplasia (63.2%, 24/38), and cerebellar microcysts (57.9%, 22/38) were the most prevalent findings, followed by polymicrogyria-like (50%, 19/38).

The imaging groups were defined as follows (Figure 2): **Group 1 (n=19)** was defined by combined supratentorial and infratentorial anomalies. Supratentorial involvement was universal (100.0%, 19/19), dominated by polymicrogyria-like (94.7%, 18/19) and cortical thickening (84.2%, 16/19), which typically showed an anterior-posterior gradient (89.5%, 17/19). All patients (100.0%, 19/19) presented with concurrent infratentorial defects, featuring a thin brainstem (100.0%, 19/19), cerebellar dysplasia (94.7%, 18/19), and/or cerebellar cysts (94.7%, 18/19). Ventriculomegaly (57.9%, 11/19) and white matter changes (84.2%, 16/19) were frequent. **Group 2 (n=9)** exhibited malformations isolated to the posterior fossa. Cerebellar dysplasia was universal (100.0%, 9/9), accompanied by brainstem hypoplasia in 55.6% (5/9) of cases and cerebellar microcysts in 44.4% (4/9). **Group 3**

(n=10) comprised patients with either normal MRI scans (30.0%, 3/10) or isolated non-specific changes (70.0%, 7/10), such as punctate white matter abnormalities 60% (6/10)or mild ventriculomegaly 20% (2/10), in the absence of definitive cortical or posterior fossa malformations.

3.3 Clinical-Imaging Correlation Analysis

Analysis of the 63 patients with MRI records revealed a distribution consistent with clinical severity. All 23 Type A patients exhibited structural anomalies, predominantly as combined supratentorial-infratentorial 82.6% (19/23) or isolated infratentorial patterns 17.4% (4/23) . Among 28 Type B patients, brain abnormalities manifested differently based on intellectual status: patients without intellectual disability showed only infrequent cerebellar dysplasia 42.9% (3/7), while those with intellectual disability displayed heterogeneous patterns: most commonly normal/non-specific findings 47.6% (10/21), followed by predominant infratentorial involvement 28.6% (6/21), with 5 cases showing cortical involvement (including 4 combined malformations and 1 isolated anomaly). All 12 Type C patients had normal scans or non-specific findings.

Formal statistical analysis of the 38-patient imaging cohort confirmed a strong positive correlation between clinical severity type (A/B/C) and imaging group (1/2/3) (Spearman's $\rho = 0.756$, $P < 0.001$) with moderate agreement (weighted Kappa = 0.623). However, specific phenotypes demonstrated distinct patterns: MEB and LGMD clustered predominantly in Group 1 (92.3%) and Group 3 (83.3%) respectively, while CMD-MR was distributed across all groups (Group 1: 36.4%, Group 2: 27.3%, Group 3: 36.4%), indicating heterogeneity within this clinical category despite the overall correlation (Table S2 and Figure 2c).

3.4 Genotype-Specific Neuroimaging Patterns

The genetic composition of the 38-patient imaging cohort was: *POMGNT1*(12), *CRPPA* (7), *POMT1* (6), *FKRP* (5), *FKTN* (4), *POMT2* (2), and *B3GALNT2* (2) (Figure 2d). Stratified analysis revealed distinct genotype-imaging correlation patterns (Table S3).

Mutations in *POMGNT1* and *B3GALNT2* were associated with a consistent severe spectrum, where severe clinical phenotypes (MEB, FCMD) corresponded almost exclusively to the most severe imaging group (Group 1), showing a strong positive correlation ($\rho = 0.817$, $P = 0.0012$) for *POMGNT1*. Notably, 10 of 12 (83.3%) *POMGnT1* patients were classified into Group 1. In contrast, the *CRPPA* genotype was defined by a specific structural hallmark: cerebellar dysplasia were present in all 7 cases (all CMD). Within *CRPPA-DGP* patients, imaging severity (Group 1 vs. Group 2) was closely tied to the severity of expressive language development.

Severe ID (language assessment classified as A or B) was associated with Group 1, while milder ID (language assessment classified as C) was associated with Group 2, resulting in a weak positive correlation ($\rho = 0.091$, $P = 0.8457$). The *POMT1*/*POMT2* genotypes exhibited a trend of "functional-structural dissociation", While intellectual disability was a common feature, structural changes on MRI were disproportionately milder. Even patients with severe clinical diagnoses (e.g., WWS) were not classified into Group 1, yielding a moderate correlation ($\rho = 0.577$, $P = 0.2302$). The *FKRP* genotype demonstrated the broadest phenotypic heterogeneity, with the weakest clinical-imaging correlation ($\rho = 0.395$, $P = 0.5101$). This distribution pattern highlights the poor predictive value of clinical phenotype for imaging severity in *FKRP*-associated dystroglycanopathies.

3.5 Associations Between Brain Malformations and Neurodevelopmental Outcomes

Neurodevelopmental outcomes showed distinct correlation patterns with specific brain malformations (Figure 3). Motor function correlated solely with lissencephaly, exhibiting a negative association $\rho = -0.49$, $P = 0.002$. Intellectual disability was broadly associated with both supratentorial and infratentorial anomalies, with the strongest correlate being brainstem hypoplasia $\rho = 0.51$, $P = 0.001$.

Expressive language impairment demonstrated the strongest and most extensive correlations, particularly with brainstem hypoplasia $\rho = 0.82$, $P < 0.001$, white matter abnormalities $\rho = 0.72$, $P < 0.001$, and supratentorial cortical involvement $\rho = 0.70$, $P < 0.001$. However, due to the high co-occurrence between infratentorial and supratentorial malformations (all Group 1 patients had both), the $\rho = 0.82$ correlation should be interpreted as reflecting combined supra- and infratentorial pathology rather than an isolated brainstem effect. Seizure occurrence showed the strongest positive correlation with infratentorial involvement $\rho = 0.47$, $P = 0.003$, followed by cerebellar hypoplasia $\rho = 0.46$, $P = 0.004$. To disentangle the independent effects of infratentorial structures from coexisting supratentorial pathology, we further performed partial correlation analyses controlling for a composite supratentorial score.(sum of cortical thickening, polymicrogyria-like, and lissencephaly).

After controlling for supratentorial factors, the correlations between infratentorial structures (cerebellar cysts, cerebellar dysplasia, and brainstem hypoplasia) and expressive language impairment were no longer significant ($r = -0.079$ to 0.274, all $P > 0.05$) (Figure S1). Notably, cerebellar dysplasia remained significantly correlated with epilepsy ($r = 0.351$, $P = 0.033$), suggesting a potential independent contribution of cerebellar dysplasia to seizure development beyond supratentorial pathology.

Receptive language deficits exhibited a unique profile, being strongly and specifically associated only with lissencephaly $\rho = 0.62$, $P < 0.001$, while showing only marginal correlations with other features. Network analysis further highlighted expressive language as the most extensively connected clinical hub and lissencephaly as a key structural node specifically linked to receptive language.

Discussion

This study systematically characterizes the brain MRI phenotypes of a genetically confirmed Chinese dystroglycanopathy (DGP) cohort, analyzing 38 high-quality cranial MRI scans and proposing a novel neuroimaging subclassification system. We identified cerebellar microcysts (prevalence 57.9%) and brainstem hypoplasia (63.2%) as characteristic neuroimaging hallmarks of DGP, and further elucidated that the clinical-imaging correlation spectrum is fundamentally determined by genotype.

Imaging Patterns and the Novel Classification System: Although a previous study suggested that all DGP patients with structural brain abnormalities exhibit cortical involvement(4, 5), our cohort analysis revealed that some patients present with isolated cortical or isolated infratentorial structural anomalies. Based on the imaging features observed in our pediatric cohort, we proposed a novel three-tier classification system: Group 1 (combined supratentorial and infratentorial malformations), Group 2 (isolated infratentorial malformations), and Group 3 (normal or non-specific findings). This classification demonstrated a strong correlation with clinical severity ($\rho = 0.756$, $P < 0.001$), validating its utility in prognostic stratification.

Among the 38 patients, infratentorial structural abnormalities were the most prevalent, including cerebellar dysplasia (71.1%), cerebellar microcysts (57.9%), and brainstem hypoplasia (63.2%). Cerebellar cysts are relatively rare in pediatric neuroimaging.(6, 7) Beyond DGP, cerebellar cysts have been reported only in case series or sporadic reports of non-muscular disorders, including GPR56-related encephalopathy (7), Poretti-Boltshauser syndrome caused by *LAMA1* mutations (8), Aicardi syndrome (9, 10), and pontocerebellar hypoplasia type 6 (11). Therefore, the presence of cerebellar cysts on brain MRI in patients presenting with muscular dystrophy provides a strong diagnostic indication for DGP, warranting prioritized genetic testing in hypotonic children. The high prevalence of brainstem hypoplasia in our cohort further underscores the importance of evaluating infratentorial structures in DGP.

Infratentorial Structural Abnormalities: A key consideration is the frequent co-occurrence of infratentorial and supratentorial structural abnormalities in our cohort. Since all Group 1 patients had both, the unadjusted

correlations observed between infratentorial structures and language impairment cannot readily distinguish independent infratentorial effects from concomitant supratentorial factors. To address this, we further performed partial correlation analyses controlling for a composite supratentorial score (sum of cortical thickening, polymicrogyria-like, and lissencephaly). Despite this, comparison between groups reveals distinct patterns. Receptive language deficits occurred only with lissencephaly ($\rho = 0.62$, $P < 0.001$; 4/6 patients, all in Group 1); the sole exception was a Group 2 patient with Walker-Warburg syndrome who died prematurely, likely reflecting restricted developmental acquisition. Unadjusted analyses showed that expressive language impairment was significantly correlated with brainstem hypoplasia, cerebellar dysplasia, and cerebellar cysts. Group comparisons revealed that 44% of patients with isolated infratentorial malformations (Group 2) still exhibited expressive language impairment, suggesting that infratentorial abnormalities may affect language function even in the absence of overt supratentorial involvement. This observation aligns with Clement et al.(12), who noted that infratentorial structures are frequently affected in isolation in dystroglycanopathies, highlighting their vulnerability. However, our partial correlation analyses showed that these associations were no longer significant after controlling for supratentorial factors. Taken together, these findings suggest that while infratentorial abnormalities may contribute to language dysfunction, this effect is largely intertwined with—and difficult to disentangle from—coexisting supratentorial pathology, which appears to play a dominant role. The observation of language impairment in Group 2 may also reflect subtle supratentorial microstructural alterations undetectable by conventional MRI, warranting further investigation with advanced neuroimaging techniques.

From a neuropathological perspective, studies have shown that cerebellar cysts in DGP patients align along the leptomeningeal surface, likely resulting from invagination or entrapment of the subarachnoid space (13, 14), and additional evidence suggests that cerebellar histopathological changes involve abnormal lamination due to granule cell deficiency (15). Functionally, the cerebellum is involved in language processing through cerebello-cerebral loops, and prior work has confirmed that the cerebellum participates in non-motor language processing via crossed reciprocal cerebello-cerebral connections and timing/sequencing mechanisms; (16) this mechanism may explain the strong association between infratentorial structural abnormalities and expressive language impairment observed in our study. In other disorders, posterior fossa malformations (such as cerebellar hypoplasia, Joubert syndrome, and Dandy-Walker syndrome) can lead to moderate-to-severe developmental problems. (17) These parallels reinforce the critical role of infratentorial circuit integrity in language development.

Cerebellar dysplasia and epilepsy Partial correlation analysis showed that cerebellar dysplasia remained significantly correlated with epilepsy after controlling for supratentorial factor . Elder et al. (18) suggested that cerebellar lesions may contribute to epileptogenesis through disinhibition of the dentato-thalamo-cortical pathway, with the underlying mechanism involving Purkinje cell loss and subsequent disinhibition of the deep cerebellar nuclei. Therefore, in DGP patients with cerebellar dysplasia, clinical attention should be paid to monitoring for seizure activity.

Specific Association of Lissencephaly: From a neuropathological perspective, cobblestone lissencephaly represents the typical brain malformation in DGP, with the underlying mechanism being disruption of the glia limitans leading to neuroglial overmigration into the arachnoid space (15, 19). In contrast to the broad network-level associations of infratentorial abnormalities, lissencephaly demonstrated a highly specific correlation pattern. Network analysis further highlighted lissencephaly as a key structural node specifically linked to receptive language. Additionally, lissencephaly showed a significant correlation with motor dysfunction. It should be noted that motor dysfunction in DGP fundamentally originates from primary muscle pathology; the correlation between lissencephaly and motor function may reflect lissencephaly as a marker of more severe systemic disease phenotype, though the exact mechanism requires further investigation.

Genotype Dictates the Clinical-Imaging Correlation Spectrum: The clinical-imaging correlation spectrum is fundamentally determined by genotype. *POMGNT1* and *B3GALNT2* mutations were predominantly associated with severe combined malformations (Group 1), consistent with previous reports linking these genes to the most severe end of the DGP spectrum. (20, 21) In contrast to previous reports in which most *CRPPA* patients exhibited severe phenotypes (22, 23), all *CRPPA* patients (all CMD) in our cohort uniformly featured cerebellar dysplasia with imaging severity correlated with expressive language development grade. Notably, imaging severity in *CRPPA* patients showed no significant correlation with intellectual disability. *POMT1*/*POMT2* exhibited a marked "function-structure dissociation" pattern, characterized by significant intellectual disability despite disproportionately mild structural changes (mostly classified into Group 2 or Group 3), suggesting a pathophysiology affecting neuronal microcircuitry and synaptic function over macrostructure.(24) Previous studies have reported that regardless of muscle strength, brain MRI in *FKRP* patients is typically normal or shows only mild posterior fossa involvement (25), which may explain why brain MRI is rarely performed. In our cohort, most *FKRP* patients also showed relatively mild imaging changes, although one patient with CMD-MR was

classified into Group 1 (combined supratentorial-infratentorial malformations). Overall, the clinical-imaging correlation in *FKRP* mutations remained weak ($\rho = 0.395$). *FKTN* mutations, though limited in number, were consistently associated with severe phenotypes, consistent with their established role in Fukuyama congenital muscular dystrophy.(26) These findings underscore the necessity of genotype-guided precision management.

This study has limitations, including limited sample sizes for certain genotypes and the frequent co-occurrence between infratentorial and supratentorial structural abnormalities. Future studies with larger sample sizes or advanced techniques such as diffusion tensor imaging are needed to further elucidate the differential contributions of different structures.

In conclusion, this study defines genotype-specific neuroimaging signatures in dystroglycanopathy. We demonstrate that comprehension deficit is a highly specific clinical feature in DGP, strongly associated only with lissencephaly; whereas language function is the most widespread and sensitive clinical indicator. The strong correlations of brainstem hypoplasia and cerebellar abnormalities with language outcomes provide evidence for the important role of infratentorial structures in language function, though these correlations should be interpreted with caution given the collinearity limitations. The neurological sequelae of DGP arise from complex genotype-specific interactions affecting both cerebral and cerebellar development. Therefore, an integrated approach combining genetic diagnosis, detailed neuroimaging with emphasis on infratentorial structure assessment, and targeted neurodevelopmental evaluation is essential for precise prognostication and optimized patient management.

Acknowledgments

We are grateful to the patients and their families. This work was supported by Beijing Natural Science Foundation (7254435), National Natural Science Foundation of China (No. 82471430) and Open Research Fund Program of MOE Key Laboratory of Major Diseases in Children (Capital Medical University), Ministry of Education (No. BCH-MOE-2025-9).

References

1. Kanagawa M. Dystroglycanopathy: From Elucidation of Molecular and Pathological Mechanisms to Development of Treatment Methods. Int J Mol Sci. 2021;22(23).

2. Song D, Dai Y, Chen X, Fu X, Chang X, Wang N, et al. Genetic variations and clinical spectrum of dystroglycanopathy in a large cohort of Chinese patients. Clin Genet. 2021;99(3):384-95.

3. Godfrey C, Foley AR, Clement E, Muntoni F. Dystroglycanopathies: coming into focus. Curr Opin Genet Dev. 2011;21(3):278-85.

4. Brun BN, Mockler SR, Laubscher KM, Stephan CM, Wallace AM, Collison JA, et al. Comparison of brain MRI findings with language and motor function in the dystroglycanopathies. Neurology. 2017;88(7):623-9.

5. Godfrey C, Clement E, Mein R, Brockington M, Smith J, Talim B, et al. Refining genotype phenotype correlations in muscular dystrophies with defective glycosylation of dystroglycan. Brain. 2007;130(Pt 10):2725-35.

6. Angelini C, Pinzan E. Advances in imaging of brain abnormalities in neuromuscular disease. Ther Adv Neurol Disord. 2019;12:1756286419845567.

7. Poretti A, Häusler M, von Moers A, Baumgartner B, Zerres K, Klein A, et al. Ataxia, intellectual disability, and ocular apraxia with cerebellar cysts: a new disease? Cerebellum. 2014;13(1):79-88.

8. Micalizzi A, Poretti A, Romani M, Ginevrino M, Mazza T, Aiello C, et al. Clinical, neuroradiological and molecular characterization of cerebellar dysplasia with cysts (Poretti-Boltshauser syndrome). Eur J Hum Genet. 2016;24(9):1262-7.

9. Steffensen TS, Gilbert-Barness E, Lacson A, Margo CE. Cerebellar migration defects in aicardi syndrome: an extension of the neuropathological spectrum. Fetal Pediatr Pathol. 2009;28(1):24-38.

10. Hopkins B, Sutton VR, Lewis RA, Van den Veyver I, Clark G. Neuroimaging aspects of Aicardi syndrome. Am J Med Genet A. 2008;146a(22):2871-8.

11. Glamuzina E, Brown R, Hogarth K, Saunders D, Russell-Eggitt I, Pitt M, et al. Further delineation of pontocerebellar hypoplasia type 6 due to mutations in the gene encoding mitochondrial arginyl-tRNA synthetase, RARS2. J Inherit Metab Dis. 2012;35(3):459-67.

12. Clement E, Mercuri E, Godfrey C, Smith J, Robb S, Kinali M, et al. Brain involvement in muscular dystrophies with defective dystroglycan glycosylation. Ann Neurol. 2008;64(5):573-82.

13. Aida N, Tamagawa K, Takada K, Yagishita A, Kobayashi N, Chikumaru K, et al. Brain MR in Fukuyama congenital muscular dystrophy. AJNR Am J Neuroradiol. 1996;17(4):605-13.

14. Aida N, Yagishita A, Takada K, Katsumata Y. Cerebellar MR in Fukuyama congenital muscular dystrophy: polymicrogyria with cystic lesions. AJNR Am J Neuroradiol. 1994;15(9):1755-9.

15. Devisme L, Bouchet C, Gonzalès M, Alanio E, Bazin A, Bessières B, et al. Cobblestone lissencephaly: neuropathological subtypes and correlations with genes of dystroglycanopathies. Brain. 2012;135(Pt 2):469-82.

16. Mariën P, Borgatti R. Language and the cerebellum. Handb Clin Neurol. 2018;154:181-202.

17. Steinlin M. Cerebellar disorders in childhood: cognitive problems. Cerebellum. 2008;7(4):607-10.

18. Elder C, Kerestes R, Opal P, Marchese M, Devinsky O. The cerebellum in epilepsy. Epilepsia. 2025;66(6):1773-92.

19. Sharma PK, Jerosha S, Subramonian SG, Raja RS, Rk K. Cobblestone lissencephaly (Type II), clinical, and neuroimaging: A case report and literature review. Radiol Case Rep. 2024;19(11):4794-803.

20. Diesen C, Saarinen A, Pihko H, Rosenlew C, Cormand B, Dobyns WB, et al. POMGnT1 mutation and phenotypic spectrum in muscle-eye-brain disease. J Med Genet. 2004;41(10):e115.

21. Stevens E, Carss KJ, Cirak S, Foley AR, Torelli S, Willer T, et al. Mutations in B3GALNT2 cause congenital muscular dystrophy and hypoglycosylation of α-dystroglycan. Am J Hum Genet. 2013;92(3):354-65.

22. Roscioli T, Kamsteeg EJ, Buysse K, Maystadt I, van Reeuwijk J, van den Elzen C, et al. Mutations in ISPD cause Walker-Warburg syndrome and defective glycosylation of α-dystroglycan. Nat Genet. 2012;44(5):581-5.

23. Sframeli M, Sarkozy A, Bertoli M, Astrea G, Hudson J, Scoto M, et al. Congenital muscular dystrophies in the UK population: Clinical and molecular spectrum of a large cohort diagnosed over a 12-year period. Neuromuscul Disord. 2017;27(9):793-803.

24. Geis T, Rödl T, Topaloğlu H, Balci-Hayta B, Hinreiner S, Müller-Felber W, et al. Clinical long-time course, novel mutations and genotype-phenotype correlation in a cohort of 27 families with POMT1-related disorders. Orphanet J Rare Dis. 2019;14(1):179.

25. Quijano-Roy S, Martí-Carrera I, Makri S, Mayer M, Maugenre S, Richard P, et al. Brain MRI abnormalities in muscular dystrophy due to FKRP mutations. Brain Dev. 2006;28(4):232-42.

26. Ishigaki K, Taniguchi-Ikeda M. Fukuyama congenital muscular dystrophy: Clinical features and therapeutic advances. Brain Dev. 2025;47(5):104437.

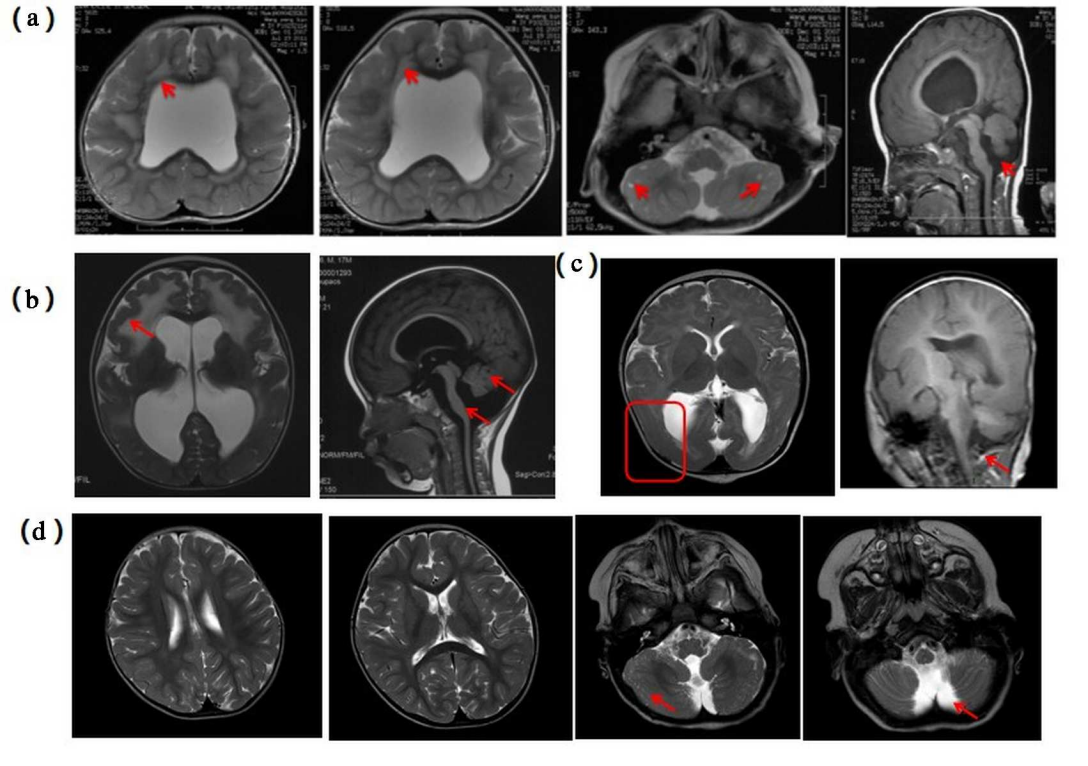
Figure legends.

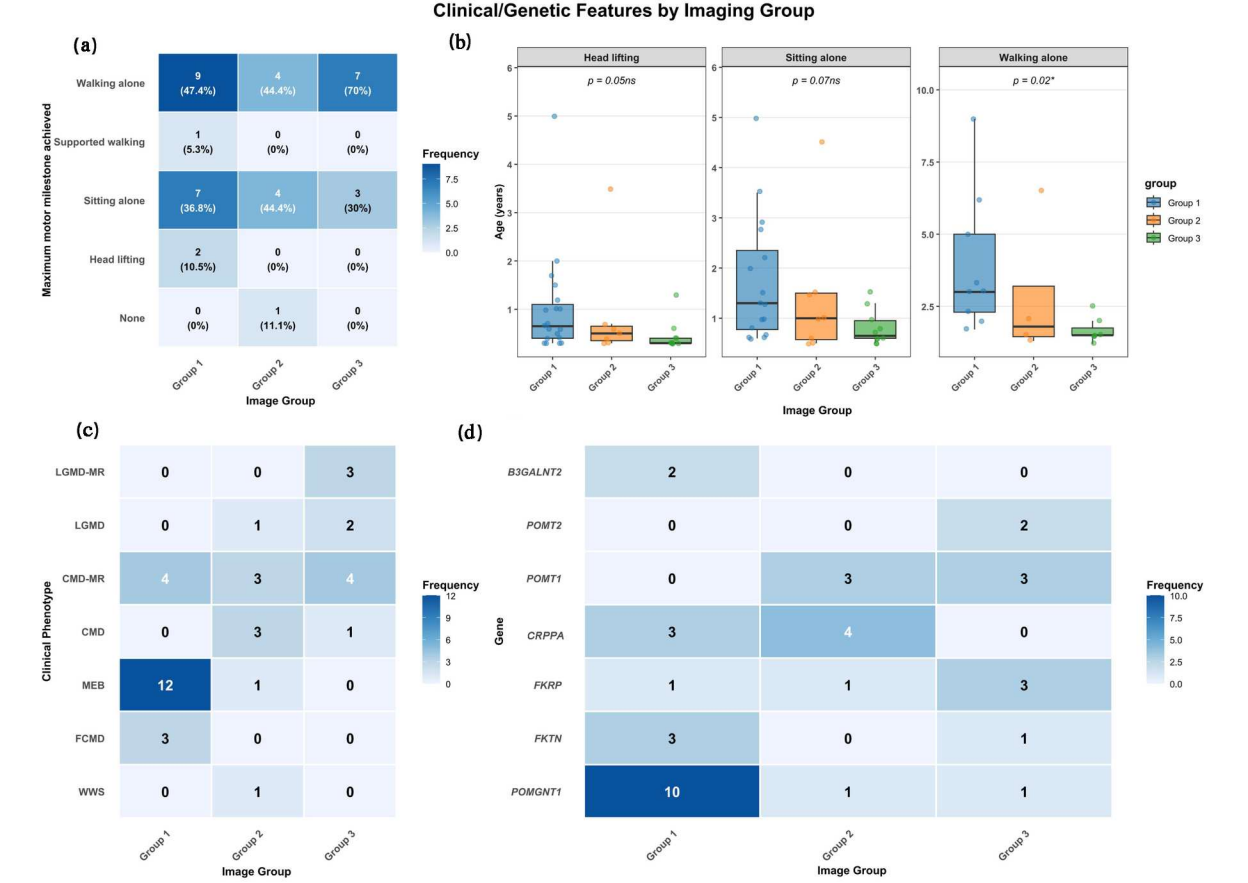
Figure 1. Representative brain MRI findings in dystroglycanopathy. (a) Group 1, Patient 5. Axial T2WI shows polymicrogyria-like (red arrow), cerebellar microcysts (red arrow), cerebellar dysplasia (red arrow), and absence of the septum pellucidum; sagittal image shows cerebellar dysplasia and brainstem hypoplasia (red arrow). (b) Group 1, Patient 12. Axial T2WI shows anterior-predominant polymicrogyria-like and white matter abnormalities; sagittal image shows cerebellar dysplasia and brainstem hypoplasia (red arrows). (c) Group 1, Patient 1. Axial T2WI shows posterior-predominant lissencephaly (red box); sagittal image shows cerebellar dysplasia and brainstem hypoplasia (red arrows). (d) Group 2, Patient 25. Axial T2WI shows no obvious supratentorial abnormalities; sagittal image shows isolated cerebellar dysplasia (red arrow) in the infratentorial region, with no brainstem hypoplasia or cerebellar microcysts.

Figure 2. Clinical/Genetic features across imaging groups. (a) Heatmap showing the distribution of the maximum motor milestone achieved in each imaging group. Numbers in each cell indicate the count (with percentage in parentheses). Color intensity reflects frequency, with darker blue representing higher counts. (b) Boxplots (median, interquartile range, range) overlaid with jittered individual data points depicting the age (years) at attainment of three motor milestones: head lifting, sitting alone, and walking alone, stratified by imaging group. P-values from Kruskal-Wallis tests comparing the three groups are shown above each facet (***p<0.001, **p<0.01, *p<0.05, ns not significant). (c) Heatmap illustrating the frequency of clinical phenotypes across imaging groups. Phenotypes are ordered from most severe (WWS) to mildest (LGMD-MR) based on clinical severity. (d) Heatmap displaying the frequency of causative genes across imaging groups. For all heatmaps, the color scale (blue gradient) represents frequency.

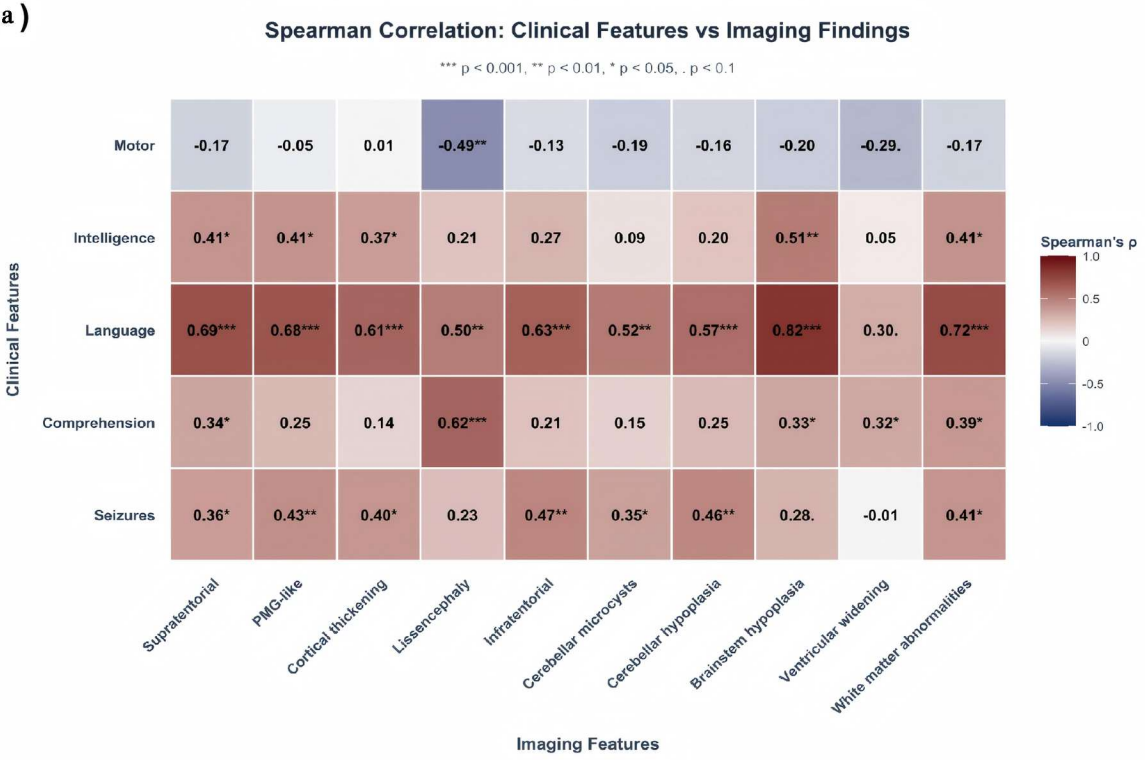
Figure 3. Spearman correlation heatmap and network analysis of clinical features versus brain malformations. (a) Heatmap showing Spearman's rank correlation coefficients (ρ) between five clinical domains (Motor, Intelligence, Language, Comprehension, Seizures) and ten imaging features. The color scale ranges from dark blue (negative correlation) through white (no correlation) to dark red (positive correlation). Correlation values are displayed within each cell, with asterisks indicating statistical significance (*$p < 0.05$, **$p < 0.01$, ***$p < 0.001$; dots indicate $p < 0.1$). (b) Correlation network illustrating significant associations ($|\rho| > 0.4$, $p < 0.05$). Nodes represent clinical (blue) and imaging (green) variables, with node size proportional to weighted degree (sum of absolute correlation strengths). Edges are colored by correlation direction (red = positive, blue = negative) and

width reflects the absolute ρ value. The network highlights the central role of expressive language and its widespread connections with multiple imaging features, as well as the specific association between receptive language and lissencephaly. Note: In this figure, "Language" refers to expressive language impairment, and "Comprehension" refers to receptive language deficits (ability to follow simple commands).

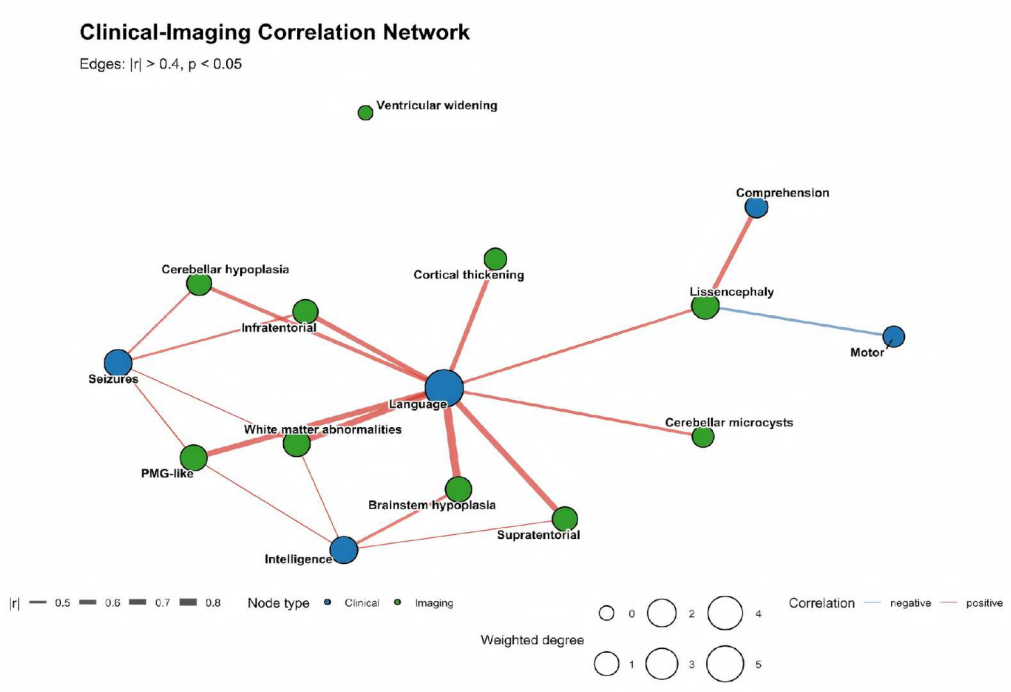

(a)
(b)
(c)
(d)


Clinical/Genetic Features by Imaging Group
(a)
Maximum motor milestone achieved
Walking alone
Supported walking
Sitting alone
Head lifting
None
9 (47.4%)
4 (44.4%)
7 (70%)
1 (5.3%)
0 (0%)
0 (0%)
7 (36.8%)
4 (44.4%)
3 (30%)
2 (10.5%)
0 (0%)
0 (0%)
0 (0%)
1 (11.1%)
0 (0%)
Group 1
Group 2
Group 3
Image Group
Frequency
7.5
5.0
2.5
0.0
(b)
Head lifting
Sitting alone
Walking alone
p = 0.05ns
p = 0.07ns
p = 0.02*
Age (years)
group
Group 1
Group 2
Group 3
Image Group
(c)
Clinical Phenotype
LGMD-MR
LGMD
CMD-MR
CMD
MEB
FCMD
WWS
0 0 3
0 1 2
4 3 4
0 3 1
12 1 0
3 0 0
0 1 0
Frequency
12
9
6
3
0
Image Group
(d)
Gene
B3GALNT2
POMT2
POMT1
CRPPA
FKRP
FKTN
POMGNT1
2 0 0
0 0 2
0 3 3
3 4 0
1 1 3
3 0 1
10 1 1
Frequency
10.0
7.5
5.0
2.5
0.0
Image Group

(a)


Spearman Correlation: Clinical Features vs Imaging Findings
*** p < 0.001, ** p < 0.01, * p < 0.05, . p < 0.1
Clinical Features
Motor -0.17 -0.05 0.01 -0.49** -0.13 -0.19 -0.16 -0.20 -0.29. -0.17
Intelligence 0.41* 0.41* 0.37* 0.21 0.27 0.09 0.20 0.51** 0.05 0.41*
Language 0.69*** 0.68*** 0.61*** 0.50** 0.63*** 0.52** 0.57*** 0.82*** 0.30. 0.72***
Comprehension 0.34* 0.25 0.14 0.62*** 0.21 0.15 0.25 0.33* 0.32* 0.39*
Seizures 0.36* 0.43** 0.40* 0.23 0.47** 0.35* 0.46** 0.28. -0.01 0.41*
Supratentorial
PMG-like
Cortical thickening
Lissencephaly
Infratentorial
Cerebellar microcysts
Cerebellar hypoplasia
Brainstem hypoplasia
Ventricular widening
White matter abnormalities
Imaging Features
Spearman's ρ
1.0
0.5
0
-0.5
-1.0

(b)


Clinical-Imaging Correlation Network
Edges: |r| > 0.4, p < 0.05
Ventricular widening
Comprehension
Cerebellar hypoplasia
Cortical thickening
Lissencephaly
Infratentorial
Motor
Seizures
Language
White matter abnormalities
Cerebellar microcysts
PMG-like
Brainstem hypoplasia
Supratentorial
Intelligence
|r| 0.5 0.6 0.7 0.8
Node type Clinical Imaging
Weighted degree 0 1 2 3 4 5
Correlation negative positive

Supplementary Files

This is a list of supplementary files associated with this preprint. Click to download.

- Table1.docx
- Table2.docx
- TableS1.docx
- TableS2docx.docx
- FigureS1.tif
- TableS3.docx